

Laboratory evaluation of the geogrid effect on bed reaction coefficient in reinforced pavements

Mehdi Mansouri

MSc of civil engineering. Geo technical engineering. Islamic Azad University. Sepidan Branch. Sepidan, Iran

Roozbeh Agha Majidi

Professor Assistant. Civil Engineering Department. Islamic Azad University. Sepidan Branch. Sepidan, Iran email:

Mohammad Mansouri

MSc of civil engineering. Geo technical engineering. Islamic Azad University. Sepidan Branch. Sepidan, Iran

ABSTRACT

The present study aimed to investigate the geogrid effect on bed reaction coefficient in reinforced pavements. The geogrid effects on the bed reaction coefficient of the Vahdat intersection project in Shiraz have been studied. For this purpose, first, the required base and subbase materials with the necessary specifications for paving the road are prepared and placed inside the designed box with dimensions of $0.5 \times 0.5 \times 0.5$ m, then, the required density is obtained with the optimum moisture content and finally plate loading test with a diameter of 20 cm was performed on the fabricated samples. The results of plate loading experiments show that the presence of geogrid in the soil increases the reaction coefficient of the soil bed and ultimately increases the bearing capacity of the soil. According to the loading experiments performed on several samples with the different numbers of geogrid layers, it can be concluded that the number of layers and the location of the geogrid in the soil have a significant effect on the soil bed reaction coefficient. Comparing the results obtained from experiments performed with multiple geogrid layers, observing between the states of one, two, and three layers of geogrid, the best case in increasing the bed reaction coefficient is the state of two layers of geogrid in the soil. From the diagrams of changes in bed reaction coefficient in terms of stress at each stage of loading, it can be seen that the amount of KS increases with increasing stress at the beginning of loading and then decreases

Key words: Geogrid, Bed reaction coefficient, Reinforced pavements, Vahdat intersection project of Shiraz city

INTRODUCTION

One of the methods of mechanical stabilization and soil reinforcement is using tensile elements such as geogrid. Over the last 40 years, many geotechnical structures worldwide have been built using reinforced soil techniques and operated well (Kryukova et al., 2021; Kubanov et al., 2019; Ibrahim et al., 2019). Geo synthetics can be used in various parts of the pavement to cover its weaknesses. Their two main roles are as a separator, filters to prevent mixing of fine-grained and coarse-grained layers, and as a reinforcement to control the strains that cause failure. These materials can be used in new pavements or covers.

The continuous increase of traffic volume and axial loads on road pavements has also caused the need to reinforce and strengthen road networks. The stress applied horizontally between the structural layers of roads causes cracks in their structure, which is caused by horizontal forces and relative subsidence, and gradually these cracks cause a fracture in the asphalt layers. For this reason, reinforcement is one of the methods that can be considered to improve the performance of the pavement. Reinforcement usually involves a combination of specific materials with specific properties and characteristics within materials that do not have those properties (Bereg, 2000).

The main role of geogrids in reinforcing asphalt is to increase the tensile strength of asphalt. The weakness of asphalt against traction causes the cracks that have formed in the underlying layers of the road structure to be transferred to its surface and cause pavement damage.

Jorenby and Hicks investigated the separation mechanism in high-strength pavements. They found that the efficiency of geotextiles as separators and their effect on the pavement structure depends to a large extent on the substrate material, amount, and the number of loads along with road service life and environmental conditions. (Quoted by Hosseini 2011) Hilburton et al. found that the stress conditions in the asphalt surface and the base are similar to the stress in beam loading under load. Due to bending, the asphalt surface and the base are exposed to compressive stresses at the top and tension at the bottom. Low-viscosity materials have low tensile strength and generally depend on the lateral entrapment in the substrate (quoted by Zornberg 2011).

Instead of assuming a deformed geotextile geometry due to the groove caused by the vehicle wheel, Selmeijer et al. performed an analysis based on structural membrane theory. Their solution satisfies the forces equilibrium law in the geotextile and subgrid layers. Ignoring membrane reinforcement and emphasizing the correct position of the geotextile to apply maximum locking is a design method proposed by Haliburton (quoted by Makarchian 2009). Al-Qadi and Chair also performed a series of large-scale

experiments and concluded that the use of nonwoven needle geotextiles creates the lowest groove depth in the pavement, and these materials separate the base layer and the substrate well.

Giroud and Noiray (1981) concluded that the bearing capacity of the soft pavement bed would be equal in the unreinforced state and equal to the maximum bearing capacity in the reinforced state, ie. $q_r = (\pi + 2)C_u$. C_u is the shear strength of non-drained clay. By defining the maximum load-bearing capacity ratio in the reinforced-to-unreinforced state, Giroud and Noiray proposed that the load-bearing increase is 1.6. (Quoted by Moayedi, 2009) Similar studies have been performed by Steward et al., Barenberg (1980), and Miligan et al. (1989). In these methods, increasing the bearing capacity in the reinforced to the unreinforced state has been proposed equal to 1.7, 1.8, and 2, respectively. (Quoted by Ziaei 2006).

Roa et al. reported the results of a series of (laboratory tests) CBR experiments (saturated and unsaturated) on silty sand (SM) reinforced with randomly distributed polypropylene cloths. The experiment results showed that the amount of CBR in the soil increases significantly with increasing the number of polymer fibers. (Cited by Abdi 2010) Coleman and Austin showed that geosynthetics are suitable for consolidating and reinforcing grain layers made on weak soils and the separation performance of these geosynthetics is also remarkable. (Cited by Zorg 2011) Sprague (2006) showed that using geotextiles with hot asphalt pavement is economically justified in comparison with other alternatives in this field. (Quoted from Sarika 2011)

Generally, due to the increasing development of polymeric materials such as geogrids as a tensile element for soil reinforcement, there is a need to study reinforced soil issues to clarify its various dimensions. Especially despite laboratory and numerical research, there are still many ambiguities about how to model reinforced soil environments under different conditions and how they behave. Due to the increasing use of new materials, such as geogrids in construction projects and road construction, and the impact on increasing bearing capacity, this study investigates the geogrids effect on the reaction coefficient of beds in reinforced pavements.

RESEARCH METHODS

In this research, the geogrid effect on the bed coefficient (KS) of reinforced pavements has been investigated in a laboratory. So, the geogrid effects on the reaction coefficient of base and subbase materials of the Shiraz Vahdat intersection project have been studied. For this purpose, first, the required base and subbase materials with the necessary specifications for paving the road are prepared and placed inside the designed box with dimensions of $0.5 \times m0.5 \times m 0.5$. With the optimum moisture content, the required density is obtained, and finally, a 20 cm diameter plate loading test was performed on the fabricated samples, and the results were interpreted. The results of the experiments are drawn on suitable tables and graphs, and the geogrid effects on the reaction coefficient of granular soils are investigated. The experiments performed in this study included field and laboratory experiments, all of which were performed under the 2002ASTM standard.

Preliminary tests

This section introduces the sample quality control tests in accordance with ASTM standards.

1. Granulation test

This test was performed based on the ASTM-D421 standard on the base and subbase materials, and its results are presented in tables (1) and (2), which are based on the ASTM-D2487 standard in GW-GM unified classification system (fine-grained silt sand).

Table 1: Granulation test sieves

subbase granulation test results		
Sieve No	Percentage of passing soil	Particle size (mm)
21.2	100.00	63.500
2	98.000	50.800
1	86.00	25.400
3.8	56.00	9.520
4	41.00	4.760
10	27.00	2.000
40	14.00	0.425
200	8.00	0.075

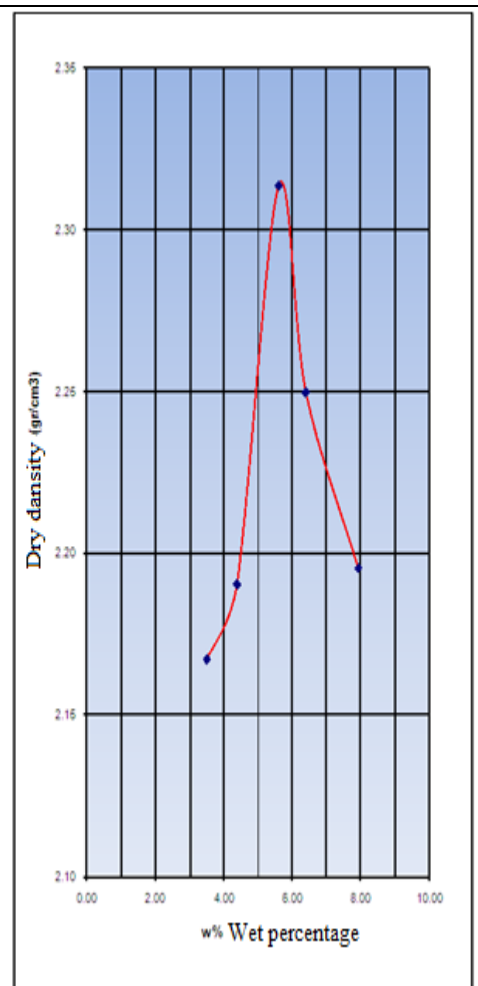
Table 2: subbase granulation curve

base granulation test results		
Sieve No	Percentage of passing soil	Particle size (mm)
11.2	100.00	38.100
1	96.000	25.400
3.4	88.00	19.100
3.8	67.00	9.520
4	48.00	4.760
10	26.00	3.000
40	12.00	0.425
200	6.00	0.075

2. Density test

This test was performed according to the ASTM D698 standard on base and subbase materials.

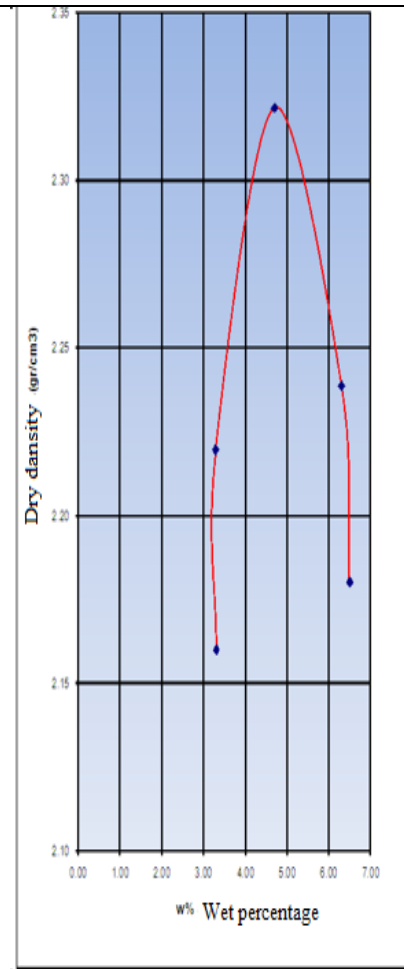
Project: Density testing of subbase materials test date:24.04.1014						
Specifications:		Sieve: 3.4	mold volume (gr):2.120		mold weight(g): 5.440	
Test results:		Maximum dry density (gr/cm2): 2.31		Optimal moisture content:5.7		
Descripti on	Unit	Values				
water volume	Cm2	200	170	140	110	80
Wet soil weight	Gr	10.195	10.287	10.620	10.515	10.463
Mold weight	Gr	5.440	5.440	5.440	5.440	5.440
wet soil weight	Gr	4.755	4.847	5.180	5.075	5.023
wet density	Gr/cm 2	2.24	2.29	2.44	2.39	2.37
Specifications of the first sample						
Descripti on	unit	values				
Can number		42	17	39	6	1
Wet soil weight, Can	Gr	83980	925.90	886.50	931.30	860.70
Dry soil weight, Can	Gr	813.90	89180	842.00	880.30	801.40
Can weight	Gr	71.30	66.80	67.50	68.90	64.40
Dry soil weight	Gr	742.60	825.00	774.50	811.40	737.00



Moisture content	Gr	25.90	34.10	44.50	51.00	59.30
Moisture percentage	%	3.49	4.13	5.75	6.29	8.05
Dry soil density	Gr/cm ²	2.17	2.20	2.31	2.25	2.19
Specifications of the second sample						
Description	unit	values				
Can number		10	22	11	7	9
Wet soil weight, Can	Gr	827.90	900.70	875.50	920.90	877.20
Dry soil weight, Can	Gr	802.10	864.10	836.20	868.70	819.50
Can weight	Gr	65.50	74.20	62.80	68.90	79.10
Dry soil weight	Gr	736.60	789.90	773.40	799.80	740.40
Moisture content	Gr	25.80	36.60	42.30	52.20	57.70
Moisture percentage	%	3.50	4.63	5.47	6.53	7.79
Dry soil density	Gr/cm ²	2.17	2.19	2.32	2.25	2.20
The average of the first and second samples						
Moisture percentage		3.50	4.38	5.61	6.41	7.92
Dry soil density	Gr/cm ²	2.17	2.19	2.31	2.25	2.20

Fig 1: Sub-base density test results

Project: Density testing of subbase materials test date: 25.2.2013						
Specification:		Sieve: 3.4	Mold volume (cm ³):2.120	Mold weight(gr):5.440		
Test results		Maximum dry density (gr/cm ²):2.32		Optimal moisture content:4.7		
Description	unit	values				
water volume	Cm ³	200	170	140	110	90
Wet soil weight	Gr	10.105	10.300	10.579	10.485	10.370
Mold weight	Gr	5.440	5.440	5.440	5.440	5.440
wet soil weight	Gr	5.665	4.860	5.139	5.045	4.930
wet density	Gr/cm ²	2.20	2.29	2.42	2.38	2.33
Specifications of the first sample						
Description	unit	values				
Can number		42	17	39	6	11
Wet soil weight, Can	Gr	904.50	890.10	855.90	938.80	875.10
Dry soil weight, Can	Gr	885.90	859.00	823.00	890.70	835.10
Can weight	Gr	71.30	66.80	67.50	68.90	62.80
Dry soil weight	Gr	814.60	792.20	755.70	821.80	772.30
Moisture content	Gr	18.60	31.10	32.70	48.10	40.00
Moisture percentage		2.28	3.93	4.33	5.85	5.18
Dry soil density	Gr/cm ²	2.15	2.21	2.32	2.25	2.21
Specifications of the second sample						
Description	unit	values				
Can number		9	22	16	9	7
Wet soil weight+ Can	Gr	940.10	878.00	865.50	937.90	880.30
Dry soil weight+ Can	Gr	894.90	857.20	839.50	883.50	836.90
Can weight	Gr	79.10	74.20	69.60	79.10	68.90
Dry soil weight	Gr	815.80	783.00	769.90	804.40	768.00
Moisture	Gr	45.20	20.80	26.00	54.40	43.40



content						
Moisture percentage		5.54	2.66	3.38	6.76	5.65
Dry soil density	Gr/cm ²	2.08	2.23	2.32	2.23	2.20
The average of the first and second samples						
Moisture percentage	%	3.30	3.29	4.70	6.31	6.50
Dry soil density	Gr/cm ²	2.16	2.22	2.32	2.24	2.18

Fig 2: Base density test results

3. Direct shear test in solidified drained conditions

This experiment aimed to determine the shear strength of compacted soil in the direct cutting machine and determine the values of adhesion (C) and internal friction angle (ϕ) of the soil in the drained state. This test is done according to ASTM D 3080 standard and with a slow shear rate (0.0025-1) mm / min on the base and subbase materials, and the results are specified in figures (3) and (4).

Direct cutting test				
Location of subbase materials project - Vahdat Intersection Project, Shiraz test date:30.06.2013				
Borehole number: BH1	research method: fast			
sample number	cutting mold dimension D=10			
sample depth	Height H=2			
tampered sample	cross-section A=100			
disturbed sample	Volume V=200			
undisturbed sample	Pre-test sample			
saturated sample	Sample number	1	2	3
unsaturated sample	Soil and mold weight	952	951	951
solidified sample	Mold weight	582	582	582
unconsolidated sample	Wet soil weight	370	369	369
saturation time: half an hour	Wet soil density (GR/CM) ²	1.85	1.85	1.85
solidification time				
Specifications of tampered laboratory samples	Natural moisture content (W)	5.4	5.4	5.4
Specific dry weight	Dry soil density (GR/CM) ²	1.76	1.75	1.75
suitable moisture content	Sample after test			
	Sample cell number			
sample No	1	2	3	cell weight

Vertical force (kg)	25	50	75	Wet soil and cell weight			
Vertical stress	0.25	0.50	0.75	Dry soil and cell weight			
Maximum shear stress	0.42	0.65	0.88	Dry soil weight			
$\Theta = 38$ degree				Water weight			
C= 0.18 kg/cm ²				Moisture percentage			

Breakage diagram of direct cutting test of subbase materials in a small box

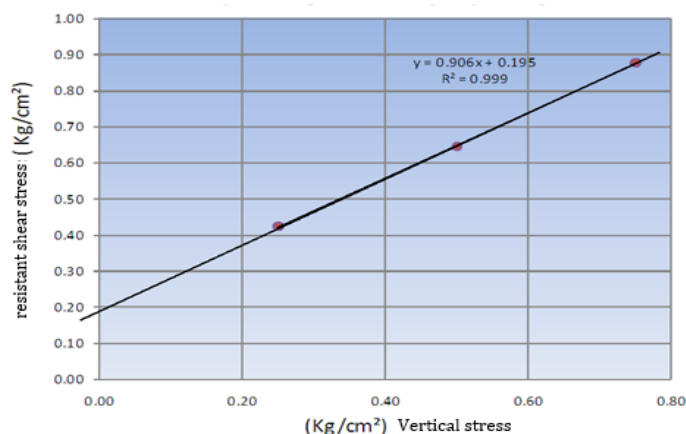


Fig3: Results of subbase direct cutting test

Direct cutting test			
Location of subbase materials project - Vahdat Intersection Project, Shiraz test date:30.06.2013			
Borehole number: BH1	research method		
sample number	cutting mold dimension D=10		
sample depth	Height	H=2	
tampered sample	cross-section	A=100	
disturbed intact sample	Volume	V=200	
undisturbed sample	Pre-test sample		
saturated sample	Sample number	1	2
unsaturated sample			3
solidified sample	Soil and mold weight	948	945
unconsolidated sample			945
saturation time: half an hour	Mold weight	582	582
solidification time			582
	Wet soil weight	366	363
			363
	Wet soil density	1.83	1.82
			1.82

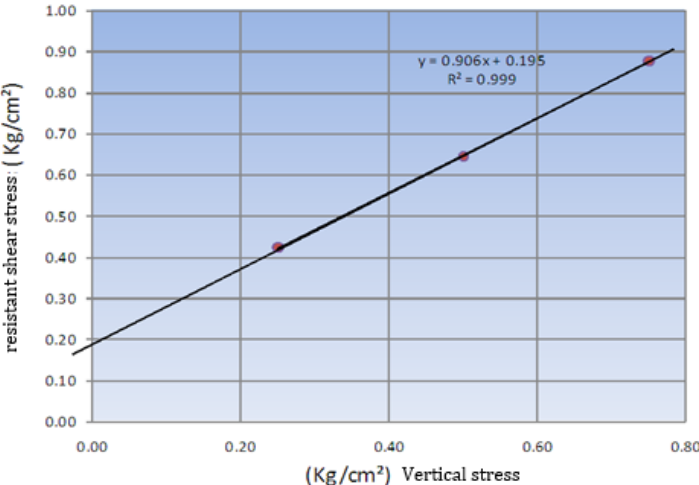
				(GR/CM) ²			
Specifications of tampered laboratory samples				Natural moisture content (W)	4.7	4.7	4.7
Specific dry weight				Dry soil density (GR/CM) ²	1.75	1.73	1.73
suitable moisture content				Sample after test			
				Sample cell number			
sample No	1	2	3	cell weight			
Vertical force (kg)	25	50	75	Wet soil and cell weight			
Vertical stress	0.25	0.50	0.75	Dry soil and cell weight			
Maximum shear stress	0.42	0.65	0.88	Dry soil weight			
Θ= 37 degree				Water weight			
C= 0.10 kg/cm ²				Moisture percentage			
Breakage diagram of direct cutting test of subbase materials in a small box							
							

Fig4: Results of base direct cutting test

4. Soil particle density test (GS)

ASTM D854 is a method for calculating the density of particles smaller than the # 4 sieve using a pycnometer.

Table 3: Results of 4. soil particle density test (GS)

Material	m ₁	m _a	m _b	K	G _s
Base	33.4	141.35	162.2	.9974	2.65
subbase	33	141.7	162.1	0.9974	2.60

5. Atterberg Limits Test include liquid limit and plastic limit tests

This experiment presents a method for determining the liquid limit, plastic limit, and soil plastic index. Atterberg Limits can be used to classify soils and identify soil properties. These tests could not be performed on the materials used due to a lack of adhesion.

6. Specifications of materials to be tested

This section presents the specifications of the materials used in the plate load test, including the base and subbase soil materials and the geogrid.

Table 4: Specifications of base and sub-base materials

Specifications	base	sub-base
Soil classification	GW-GM	GW-GM
SE	32	50
Maximum dry density (gr / cm ³)	2.31	2.32
Optimal moisture content	5.7	4.7
Internal friction angle of soil) Ø (in degrees)	38	37
Adhesion (C) (kg / cm ²)	0.18	0.1
liquid limit	indeterminable	indeterminable
plastic index	NP	NP
GS	2.65	2.6
Modulus of elasticity (ES) (kg / cm ²)	650	550

The geogrid used in this experiment is prepared by Windavar company and is of the second generation type. The second-generation geogrids are woven geogrids that 40.20 and uniaxial type has been used in this study. One of the important properties of this geogrid is the tensile strength in a length change of 2%.

Table 5: Geogrid specifications

Type of geogrid	Dimensions (mm)	Thickness (mm)	Unit weight (gr / m ²)	Tensile strength (KN / m)
Second Generation (Woven)	40*20	1.1	300	27

Plate Load Tests (PLT)

In this stage, in order to investigate the changes in the reaction coefficient of the bed due to the presence of geogrid and its placement in different positions of pavement materials, five plate load tests with a diameter of 20 cm were done on the base and subbase material with optimal moisture content, and specific gravity in the box designed with dimensions of 0.5 × 0.5 m m 0.5 m and the results were interpreted (Figure 5).

In order to design the dimensions of the test box, Plaxis 2/8 software was used to model it, and Etabas 9/2 software was used to calculate the steel sections that include the frame around the box. In this experiment, a total of 10 layers of soil with a diameter of 5 cm are compacted, of which the bottom six layers contain the subbase material (30 cm), and the top 4 layers (20 cm) contain the base material.



Fig5: Compacted materials in the box

In this experiment, the second generation is woven geogrid of 40/20 type has been used to investigate the effect of geogrid on the reaction coefficient of reinforced soil bed in road pavement and placed in different soil layers to compare its effect according to the studied data and its results. The different cases tested are as follows:

Mode 1: Geogrid at the height of 40 cm

Mode 2: Geogrid at the height of 20 cm

Mode 3: Geogrid at the height of 15 and 30 cm

Mode 4: Geogrid at the height of 15, 30, and 45 cm

Mode 5: No geogrid

After preparing the test box, the page loading device was prepared. Initially, to better distribute the stress at the location of the loading plate, cement with a thickness of 5 mm is poured under it. Then a loading plate with a diameter of 20 cm was placed on it, and a jack piston was placed on top of it. A pulley is mounted on it to control the overturning of the cylinder (Figure 6).



Fig6: Equipment used for test

According to ASTM standard, loading steps should be done in several stages, and the increase in load in each step should not be more than 95 kpa or 0.1 of the estimated load capacity. Also, loading should be static without impact and oscillation and eccentricity of the load. The load should also be kept until the subsidence has stopped or the rate of increase of the eccentricity of the load has not been fixed, although this time should not be less than 15 minutes.

In this experiment, loading was performed in 8 stages, which in each stage after stopping and reducing the subsidence rate of loads: (0.5 - 1 - 1.5 - 2 - 2.5 - 3-5 - 4-5) kg/cm² were placed on the samples. After completing each stage of the tests, the box is emptied, and new materials are replaced again.

Performing on-site specific gravity tests and testing the moisture content of several samples after the test leads to greater assurance on the dry density of the compacted soil in the test box and its moisture content.

FINDINGS

The soil bed reaction coefficient indicates the reaction between the foundation and the soil beneath it. The soil bed reaction coefficient is obtained from the stress-subsidence relationship. First, we compare the reaction coefficient of the soil bed in the presence of a geogrid layer at two different heights; as shown in Fig(7), the bed reaction coefficient at each stage of loading is determined separately. These two modes are not much different from each other, but considering that the reaction coefficient is higher in the layer mode at the height of 20 cm, it can be said that it has a more desirable mode. Since the sample has less

subsidence, in this case, it is clear that the presence of geogrid at the height of 20 cm has a greater effect on reducing sample subsidence.

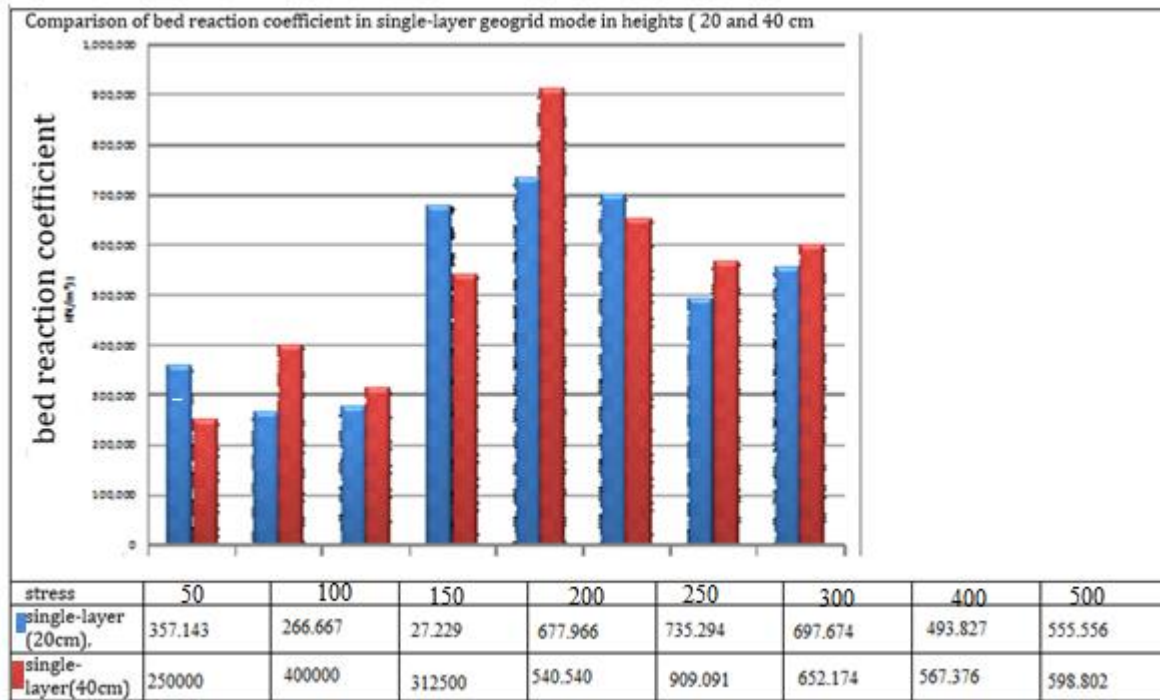


Fig7: Comparison of bed reaction coefficient in a single-layer geogrid mode

In Figures (8) and (9), the state of a geogrid layer is compared with non-geogrid mode, in which the effect of geogrid on the bed reaction coefficient in all loading stages is positive and reduces the sample subsidence.

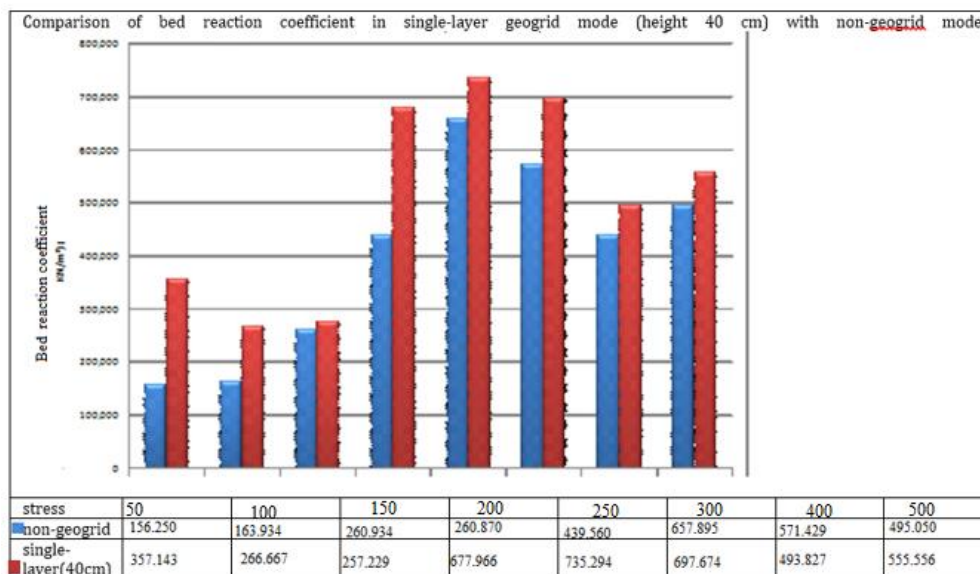


Fig 8: Comparison of bed reaction coefficient in single-layer geogrid mode (height 40 cm) with non-geogrid mode

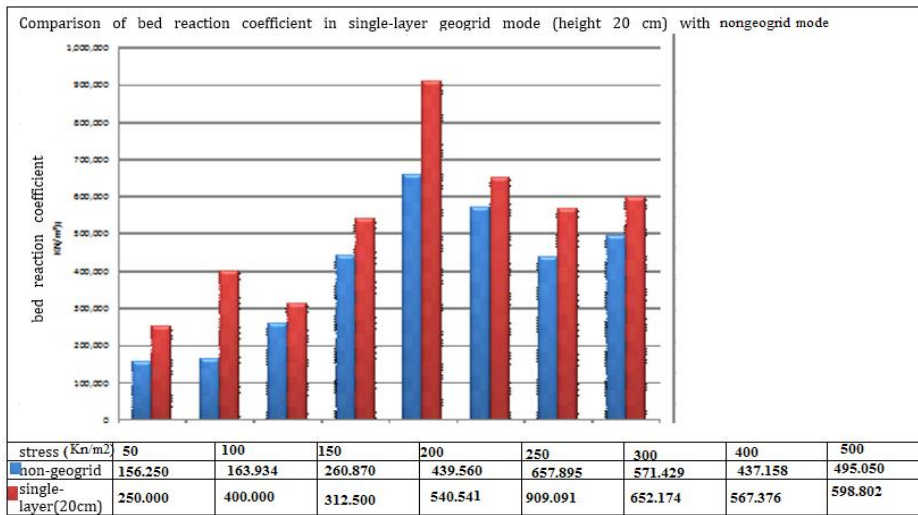


Fig 9: Comparison of bed reaction coefficient in single-layer geogrid mode (height 20 cm) with non-geogrid mode

In Figures (10) and (11), the two- and three-layer geogrid modes are compared with the non-geogrid mode, where the effect of geogrids on the bed reaction coefficient in all loading stages is positive and reduces the sample settling.

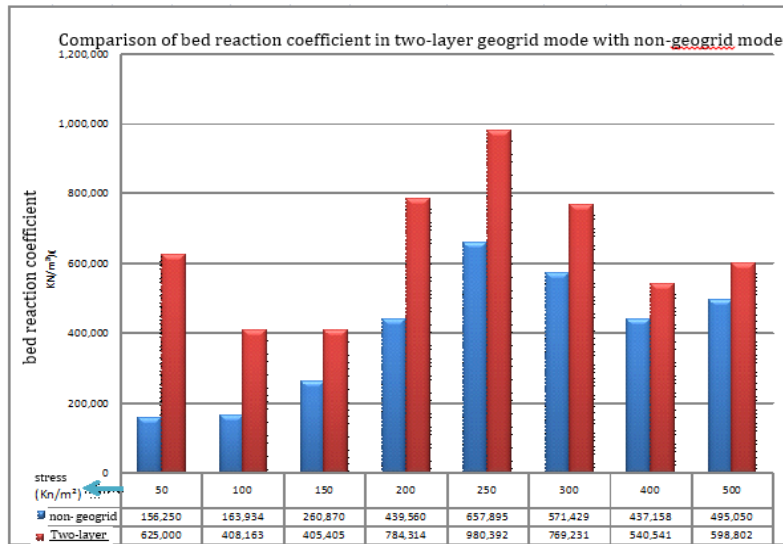


Fig 10: Comparison of bed reaction coefficient in two-layer geogrid mode with non-geogrid mode

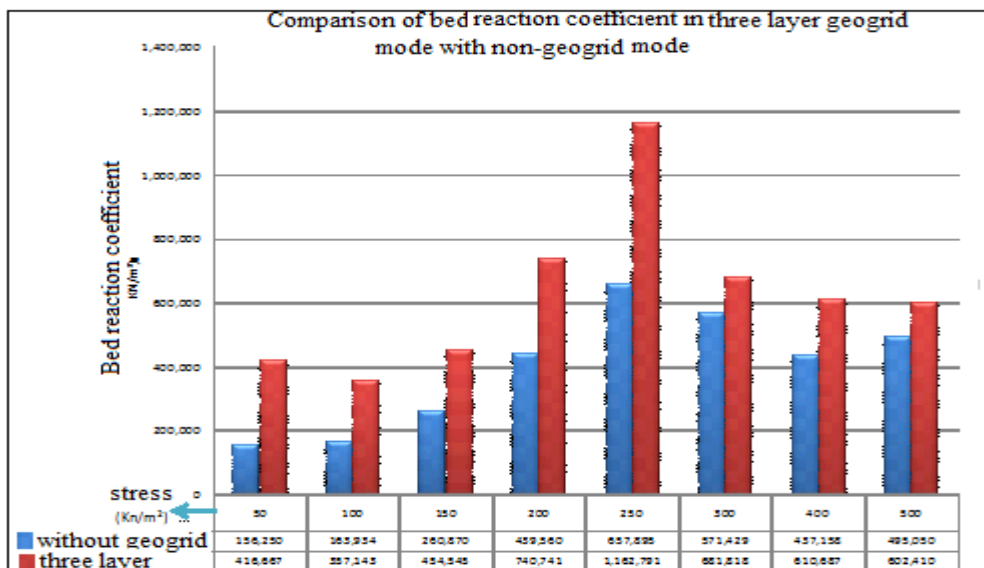


Fig 11: Comparison of bed reaction coefficient in three-layer geogrid mode with non-geogrid mode

After comparing the modes of existence of geogrid layers and non-geogrid, now we compare the modes of existence of geogrids and try to determine the most appropriate mode in terms of greater impact on the soil bed reaction coefficient. Figures (12) and (13) compare the single-layer with two and three-layer mode and show the effect of geogrid on the bed reaction coefficient in two and three-layer geogrid mode in all loading stages more and more desirable and thus reduces further subsidence in the sample.

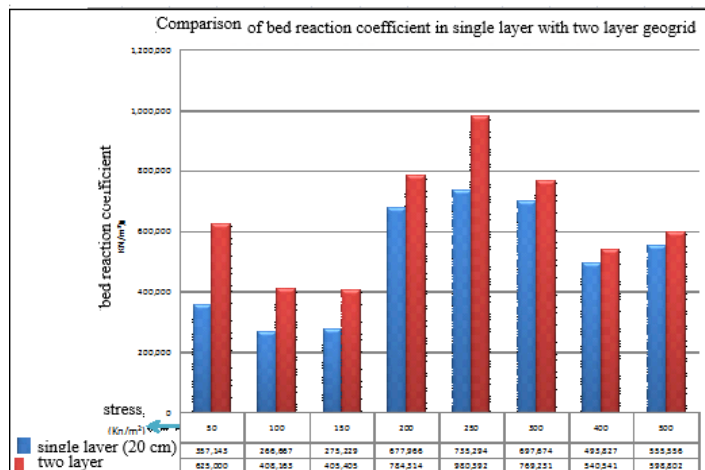


Fig12: Comparison of bed reaction coefficient in a single layer with two-layer geogrid

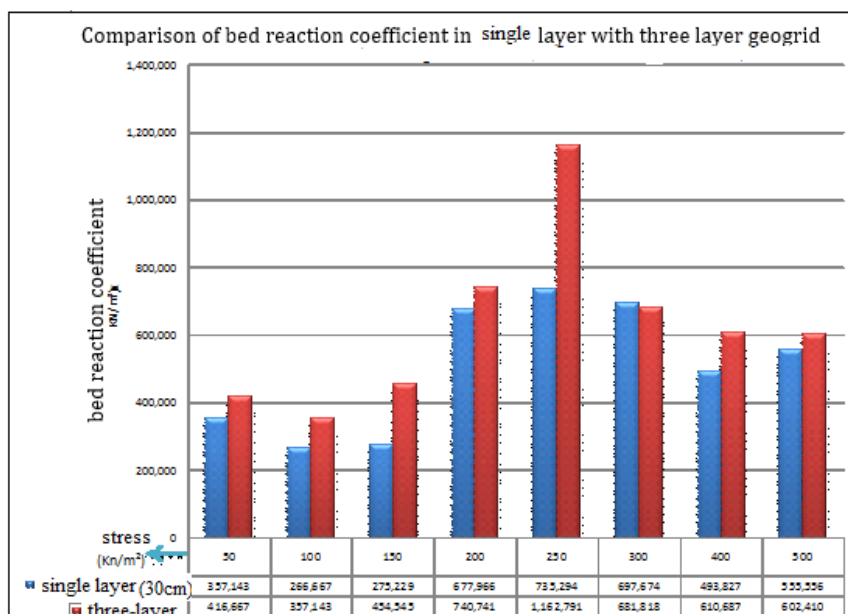


Fig13: Comparison of bed reaction coefficient in a single layer with three-layer geogrid

Finally, we will compare the two-layer and three-layer geogrid modes. According to Figure (14), it is clear that in performing eight loading steps, the impact of the geogrid in the two-layer geogrid mode in 5 steps was more than the three-layer mode. Economically, the two-layer mode also seems to be the most appropriate.

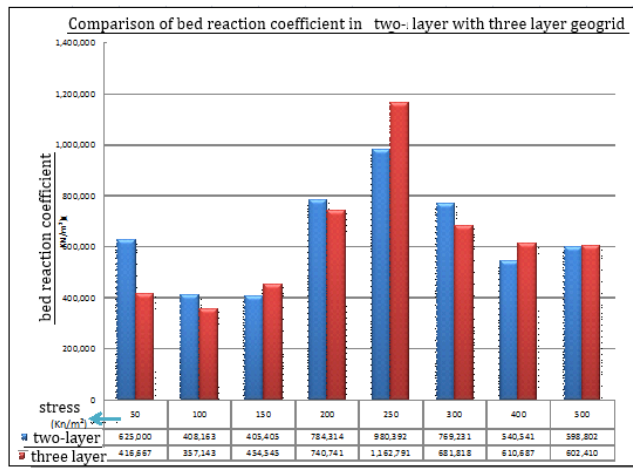


Fig14: Comparison of bed reaction coefficient in two-player mode with the three-layer mode of geogrid

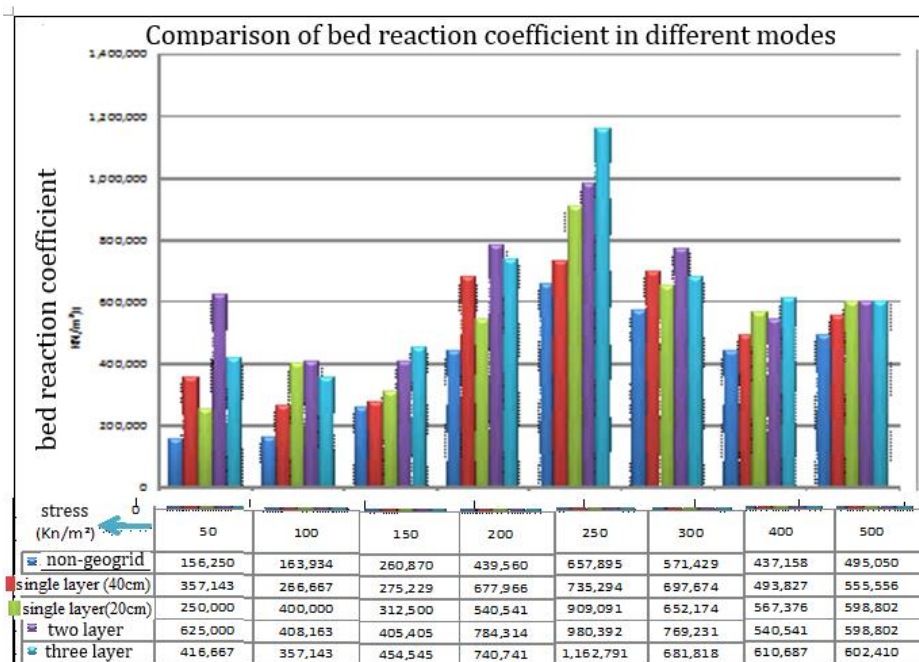


Fig15: Comparison of bed reaction coefficient in different modes

CONCLUSION

The results of plate loading experiments show that the presence of geogrid in the soil increases the soil bed reaction coefficient and ultimately increases the bearing capacity of the soil. According to the loading experiments performed on several samples with a different number of geogrid layers, it can be concluded that the number of layers and the location of the geogrid in the soil have a significant effect on the soil bed reaction coefficient. Comparing the results obtained from experiments performed with multiple layers of geogrid, observing different modes of one, two, and three layers of geogrid, the best case in increasing the bed reaction coefficient is the mode with two layers of geogrid in the soil. The diagrams show the changes in the bed reaction coefficient in terms of stress at each stage of loading, and it can be seen that the value of KS increases and then decreases with increasing stress at the beginning of loading. This is because at the beginning of loading, with increasing loading at each stage, the soil becomes denser and increases the hardness and thus increases the KS, but after the soil is broken, this hardness also decreases, and as a result, the amount of KS also decreases.

References

1. Jamileh Sadat Hosseini Saber (1390). Investigation of increasing the bearing capacity of mixed granular reinforced soils by geotextile by CBR experiment. Master Thesis - Tafresh University
2. Massoud Makarchian, Jahangir Eliassy (2009). Investigating the effect of geotextiles on increasing pavement load. 8th International Congress of Civil Engineering. May 2009 Shiraz University.
3. Hossein Moayedi, Mehdi Ebadi, Ali Torabi Haghighi (2009). Geosynthetically without reinforced pavement road design diagrams. 8th International Congress of Civil Engineering.
4. Mahmoud Reza Abdi, Mohammad Ali Arjomand, Mehdi Siavashnia (2010). Evaluation of the effect of geogrid tensile strength on soil-geogrid interaction, Fifth National Congress of Civil Engineering
5. Jorge G. Zornberg (2011). Advances in the Use of Geosynthetics in Pavement Design, The University of Texas at Austin, USA / President, International Geosynthetics Society, Geosynthetics India'11, 23-24 September 2011, IIT Madras, Chennai.
6. Sarika B. Dhule, S.S. Valunekar , S.D. Sarkate , S.S. Korrane (2011). Improvement of Flexible Pavement With Use of Geogrid. Government College of Engineering, Aurangabad (M.S), India. Vol. 16 [2011], Bund. C
7. Ziaie Moayed , R.Naeini,S,A,(2006).Evaluation of moduld of Subgrade reacyion (KS) in gravely soils based on SPT results.IAEG paper number 505 The Geological Society of London.
8. Jorge G. Zornberg (2011). Advances in the Use of Geosynthetics in Pavement Design, The University of Texas at Austin, USA / President, International Geosynthetics Society, Geosynthetics India'11, 23-24 September 2011, IIT Madras, Chennai.
9. Berg RR, Christopher BR, Perkins SW (2000), Geosynthetic Reinforcement of the Aggregate Base Course of Flexible Pavement Structures, GMA White Paper II, Geosynthetic Materials Association, Roseville, MN, USA, p. 130
10. Al-Qadi I, Baek J (2008). Mechanism of Overlay Reinforcement to Retard Reflective Cracking under Moving Vehicular Loading. Pavement Cracking. CRC Press, pp. 56.74.
11. Kryukova, E. M., Khetagurova, V. S., Ilyin, V. A., Chizhikova, V. V., & Kosoplechev, A. V. (2021). Forming students' environmental culture: modern educational approaches and technologies. *Journal of Advanced Pharmacy Education & Research*, 11(2), pp. 113-118
12. Kubanov, S. I., Savina, S. V., Nuzhnaya, C. V., Mishvelov, A. E., Tsoroeva, M. B., Litvinov, M. S., ... & Povetkin, S. N. (2019). Development of 3d bioprinting technology using modified natural and synthetic hydrogels for engineering construction of organs. *International Journal of Pharmaceutical and Phytopharmacological Research*, 9(5), pp. 37-42.
13. Ibrahim, S., Azhar, A. S., Ather, A. S., Ahsan, A. S., Muneer, A. S., & Kaleem, A. S. (2019). Backache: association with stature, posture and work-station ergonomics in information technology professionals-an analytical study. *International Journal of Pharmaceutical Research & Allied Sciences*, 8(2), pp. 10-14